ELSEVIER

Colloids and Surfaces
A: Physicochemical and Engineering Aspects 206 (2002) 349–361

COLLOIDS AND SURFACES A

www.elsevier.com/locate/colsurfa

Monolayer spreading on a chemically heterogeneous substrate

N. Pesheva [a,*], G. Oshanin [b]

[a] *Institute of Mechanics, Bulgarian Academy of Sciences, Acad. G. Bonchev St. 4, 1113 Sofia, Bulgaria*
[b] *Laboratoire de Physique Théorique des Liquides, Université Paris 6, 4 Place Jussieu, 75252 Paris, France*

Abstract

We study the spreading kinetics of a monolayer of hard-core particles on a semi-infinite, chemically heterogeneous solid substrate, one side of which is coupled to a particle reservoir. The substrate is modeled as a square lattice containing two types of sites—ordinary ones and special, chemically active sites placed at random positions with mean concentration α. These special sites temporarily immobilize particles of the monolayer which then serve as impenetrable obstacles for the other particles. In terms of a mean-field-type theory, we show that the mean displacement $X_0(t)$ of the monolayer edge grows with time t as $X_0(t) = \sqrt{2D_\alpha t \ln(4D_\alpha t/\pi a^2)}$, ($a$ being the lattice spacing). This time dependence is confirmed by numerical simulations; D_α is obtained numerically for a wide range of values of the parameter α and trapping times of the chemically active sites. We also study numerically the behavior of a stationary particle current in finite samples. The question of the influence of attractive particle–particle interactions on the spreading kinetics is also addressed.

Keywords: Monolayer spreading; Chemically heterogeneous substrates; Dynamic percolation

1. Introduction

The stability and spreading kinetics of ultrathin wetting films on solid substrates are of technological and scientific importance in many applications ranging from coatings, paints, dielectric layers, thin film lubrication, microelectronic devices, to fundamental studies of adsorption and particle dynamics [1–4]. In the case of homogeneous, chemically pure substrates, the properties of such films are relatively well understood through a series of experimental and theoretical works [1–8].

However, most of the naturally occurring surfaces used in thin film experiments are chemically heterogeneous on nanometer to micrometer scales, e.g. due to contamination, cavities, uneven oxide layer, etc. On the other hand, deliberately tailored chemically heterogeneous substrates are also increasingly being used for engineering of desired nano- and micropatterns in thin films (see, e.g. Refs. [9,10]). In addition, some recent studies have revealed a possibility of controlling the growth of biological systems by attaching them to structured surfaces [11] and to recognize biological molecules, (e.g. proteins), selectively by bringing them into contact with nanostructured surfaces [12].

* Corresponding author.

0927-7757/02/$ - see front matter
PII: S0927-7757(02)00051-1

A considerable amount of recent theoretical, numerical and experimental work has been devoted to the analysis of equilibrium properties of thin films on chemically heterogeneous substrates. These studies focused mostly on such issues as stability of films, pattern formation, appearance of self-organized structures, as well as the impact of chemical disorder on the contact angle and appropriate generalization of the Young's equation [13–20]. Much less is known, however, on spreading kinetics of ultrathin liquid films on chemically disordered surfaces. Here, the only available studies concern molecular dynamics simulations [21,22] and experimental analysis [23,24] of precursor films spreading on substrates with chemically impure sites. To the best of our knowledge, no theoretical analysis has been as yet performed.

In the present paper, motivated by recent experimental studies of precursor films spreading on chemically disordered substrates [23,24], we analyse the spreading kinetics of molecularly thin films on substrates with randomly placed chemically active sites. We focus here on systems with the so-called planar geometry, i.e. on systems in which film's thickness (or concentration of particles in the film in case of monolayers) varies effectively only along one spatial coordinate. This typical experimental situation occurs when a solid, which may be a plane or a cylindrical fiber, is immersed in a liquid bath. Here, the particle concentration in the liquid film, which extracts from the macroscopic meniscus and climbs along the solid, varies only with the altitude above the edge of the macroscopic meniscus and is independent of the perpendicular, horizontal coordinate. The meniscus then serves as a reservoir of particles, which is in equilibrium with the spreading monolayer and 'feeds' it. The solid substrate is modeled here in a usual fashion as a regular, square lattice of adsorption sites; chemical heterogeneity is introduced by adding some concentration α of special, chemically active sites, which temporarily trap moving particles which then become obstacles for others. We analyse here, both analytically and numerically, the behavior of the mean displacement $X_0(t)$ of the monolayer edge. In terms of a mean-field-type approach, we find that $X_0(t)$ grows with time t as $X_0(t) = \sqrt{2D_\alpha t \ln(4D_\alpha t/\pi a^2)}$, ($a$ being the lattice spacing). This time dependence, which contains a non-trivial logarithmic factor, is confirmed by the numerical simulations. As well, we obtain D_α numerically for a wide range of values of chemical sites' concentration α and of the trapping times. We also consider the situation when our substrate is of a finite extent along the X-axis and study numerically the behavior of the stationary particle current. The question of the influence of attractive particle-particle interactions on spreading kinetics is also addressed.

The paper is structured as follows: in Section 2 we formulate a microscopic stochastic model of spreading kinetics. In Section 3 we derive basic equations and present their mean-field-type solution appropriate for situations with annealed spatial distribution of the chemically active sites. In Section 4 we describe our Monte Carlo simulations model. Results of Monte Carlo simulations of spreading kinetics of monolayers composed of hard-core particles and analysis of the behavior of the particle current in finite samples are presented in Section 5. Next, in Section 6 we consider spreading behavior in the case when the monolayer particles experience short-range, nearest-neighbor attractive interactions. Finally, in Section 7 we conclude with a summary and discussion of our results.

2. The model

As we have already remarked, our model is relevant to the following experimental situation. Suppose that a vertical solid wall is immersed in a bath of liquid. The liquid interface, which is initially horizontal, changes its shape in the vicinity of the solid wall and a macroscopic meniscus builds up. The size of the macroscopic meniscus (both horizontally and vertically) is comparable to the capillary length. After a suitable transient period an ultrathin liquid film (a monolayer) exudes from the static macroscopic meniscus and climbs up the solid wall [2]. In Ref. [6,7] a microscopic stochastic model describing spreading kinetics of molecular films on chemically

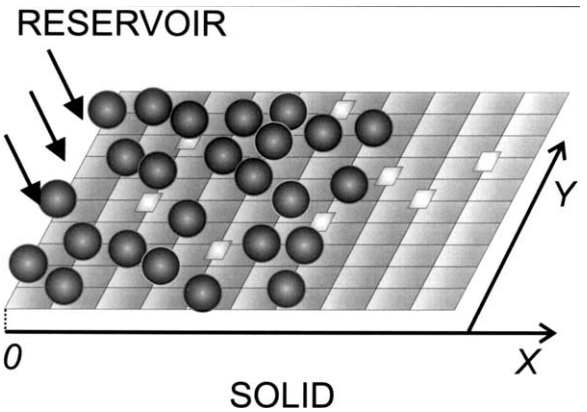

Fig. 1. Schematic representation of the monolayer in contact with a particle reservoir on a chemically heterogeneous substrate. Gray squares denote chemically active sites.

homogeneous, ideal substrates has been developed. Here we extend this approach on the situation when chemical disorder is present.

Particles dynamics on the solid surface is generally regarded as an activated random hopping motion, constrained by hard-core interactions, between the local minima of a wafer-like array of potential wells. Such wells occur because the monolayer's particles experience short-range forces exerted by the atoms of the solid. Consequently, the interwell distance a is related to the spacing between the atoms of the substrate. Without going into details of the particle–substrate interactions, we suppose that for the transition to one of the neighboring potential wells a particle has to overcome a potential barrier. This barrier does not create a preferential hopping direction, but results in a finite time interval τ between the consecutive hops, defined through the Arrhenius formula.

To specify the positions of the wells, we introduce a pair of perpendicular coordinate axes (X, Y), where X is a vertical coordinate, which measures the altitude of a given well above the meniscus (a reservoir), while Y defines the horizontal position of this well. For simplicity, we suppose that the lattice of potential wells is a regular square lattice of spacing a (see Fig. 1). It will be made clear below that the effects we observe do not drastically depend on the precise form of the underlying lattice.

Further on, we assume that the substrate contains some concentration α of immobile, chemically active sites, placed at random positions. For simplicity, we suppose that the spatial distribution of these sites is commensurate with the underlying lattice of potential wells, such that the chemically active sites can be viewed as occupying random positions on the sites of the square lattice exactly (see Fig. 1).

We turn next to the definition of the hopping probabilities. We suppose that the latter are symmetric regardless of whether a particle occupies an ordinary or a chemically active site. In the former case, a particle chooses a jump direction with the same probability equal to 1/4, which means that being on ordinary site a particle always attempts to perform a hop. On the contrary, in the latter case, there is a probability that the particle stays at the site—a pausing probability ε, which mirrors the chemical specificity of sites and hence, results in a temporal trapping effect. Here, the particle selects the jump direction with probability $(1-\varepsilon)/4$, where the parameter ε can be expressed as

$$\varepsilon = 1 - \exp(U_{\mathrm{tr}}/k_{\mathrm{B}}T) \tag{1}$$

$k_{\mathrm{B}}T$ being the temperature measured in the units of the Boltzmann constant k_{B}, while U_{tr} denotes the trapping energy, $U_{\mathrm{tr}} < 0$. Note that the typical time τ^* spent by a given particle being trapped by a chemically active site is just $\tau^* = \tau/(1-\varepsilon)$.

Consequently, the site-dependent jump direction probabilities $p(X, Y)$ can be written down as

$$p(X,Y) = \begin{cases} 1/4, & \text{if the site } (X,Y) \text{ is an ordinary site,} \\ (1-\varepsilon)/4, & \text{if the site } (X,Y) \text{ is a chemically active site.} \end{cases} \tag{2}$$

After the jump direction is chosen, the particle attempts to hop onto the target site. The jump is fulfilled if the target site is empty at this moment of time; otherwise, the particle remains at its position.

Finally, we view the liquid bath as a reservoir of particles (of an infinite capacity) which maintains a constant concentration C_0 of fluid particles at the edge of the macroscopic meniscus, i.e. the line $X=0$ in Fig. 1 (see Ref. [6,7] for more details). Here, for simplicity, we take $C_0=1$. The behavior for arbitrary C_0 will be considered elsewhere [25].

We hasten to remark that dynamics in disordered lattice gas-type models, relevant to the one employed here, has been extensively studied within different contexts, including, for instance, charge carrier transport in dynamic percolating systems [26], tracer diffusion within the first layers of solid surfaces [27] and in adsorbed monolayers [28–30], tracer and collective diffusion on solid surfaces [31,32], in pure and disordered crystals [33,34] or collective diffusion in zeolites [35–37]. The systems analyzed in these works differ, however, considerably from the situation under study; here we present a first, to the best of our knowledge, lattice gas-type description of spreading dynamics of monolayers on substrates with chemical disorder.

To close this section it might be instructive to discuss the limitations of such a non-interacting lattice-gas-type model. In the 'real world' systems, the particles appearing on top of a solid—substrate-adsorbed particles, experience two types of interactions: namely, interactions with the atoms of the underlying solid—the solid–particle (SP) interactions, and mutual interactions with each other—the particle–particle (PP) interactions. The SP interactions are characterized by a repulsion at short scales, and an attraction at longer distances. The repulsion keeps the adsorbed particles some distance apart of the solid, while attraction favors adsorption and hinders particles desorption as well as migration along the solid surface. In this regard, our model corresponds to the regime of the so-called intermediate localized adsorption [1,38]: the particles forming a monolayer are neither completely fixed in the potential wells created by the SP interactions, nor completely mobile. This means, the potential wells are rather deep with respect to the particles desorption (desorption barrier $U_d \gg k_B T$), so that only an adsorbed monolayer can exist, but have a much lower energy barrier V_1 against the lateral movement across the surface, $U_d \gg V_1 > k_B T$. In this regime, any monolayer particle spends a considerable part of its time at the bottom of a potential well and jumps sometimes, solely due to the thermal activation, from one potential minimum to another in its neighborhood; after the jump is performed, the particle dissipates all its energy to the host solid. Thus, on a macroscopic time scale the particles do not possess any velocity. The time τ separating two successive jump events, is just the typical time a given particle spends in a given well vibrating around its minimum; as we have already remarked, τ is related to the temperature, the barrier for the lateral motion and the frequency of the solid atoms' vibrations by the Arrhenius formula.

We emphasize that such a type of random motion is essentially different from the standard hydrodynamic picture of particles random motion in the two-dimensional 'bulk' liquid phase, e.g. in free-standing liquid films, in which case there is a velocity distribution and spatially random motion results from the PP scattering. In this case, the dynamics can be only approximately considered as an activated hopping of particles, confined to some effective cells by the potential field of their neighbors, along a lattice-like structure of such cells (see, e.g. Refs. [39–41]). In contrast to the dynamical model to be studied here, standard two-dimensional hydrodynamics presumes that the particles do not interact with the underlying solid. In realistic systems, of course, both the particle-particle scattering and scattering by the potential wells due to the interactions with the host solid, (as well as the corresponding dissipation channels), are important [31,42]. In particular, it has been shown that addition of dissipation to the host solid removes the infrared divergencies in the dynamic density correlation functions and thus makes the transport coefficients finite [43]. On the other hand, homogeneous adsorbed monolayers may only exist in systems in which the attractive part of the PP interaction potential is essentially weaker than that describing interactions with the solid; otherwise, such monolayers become unstable and dewet spontaneously from the solid surface. As a matter of fact, for stable

homogeneous monolayers, the PP interactions are at least ten times weaker that the interactions with the solid atoms [38].

Consequently, the standard hydrodynamic picture of particles dynamics is inappropriate under the defined above physical conditions. Contrary to that, any adsorbed particle moves due to random hopping events, activated by chaotic vibrations of the solid atoms, along the local minima of an array of potential wells, created due to the interactions with the solid [1,38]. As we have already remarked, in the physical conditions under which such a dynamics takes place, the PP interactions are much weaker than the SP interactions and hence do not perturb significantly the regular array of potential wells due to the SP interactions. In our model, we discard completely the attractive part of the PP interaction potential and take into account only the repulsive one, which is approximated by an abrupt, hard-core-type potential.

The question of the monolayer spreading in the case when some short-range attractive particle–particle interactions are present will be briefly addressed in Section 6.

3. Basic equations and a mean-field-type solution

Let $\rho_t(X,Y)$ denote the local density of the monolayer particles at time moment t at the site (X, Y). This local density obeys the following balance equation

$$\tau\frac{\mathrm{d}\rho_t(X,Y)}{\mathrm{d}t} = -p(X,Y)\rho_t(X,Y)\sum_{(X',Y')}(1-\rho_t(X',Y')) + (1-\rho(X,Y))\sum_{(X',Y')}p(X',Y') \times \rho_t(X',Y') \quad (3)$$

where (X', Y') denotes a nearest-neighboring to (X, Y) site, while the summation symbol with the subscript (X', Y') means that the summation extends over all nearest to (X, Y) sites. Note that the factors $(1-\rho_t(X',Y'))$ and $(1-\rho(X,Y))$ on the right-hand-side of Eq. (3) account for the steric constraints due to hard-core interactions and represent the (decoupled) probabilities that the target sites are unoccupied at time moment t.

Eq. (3) holds for all particles except for the rightmost particles for each fixed Y, since for the latter, by definition, the hops away of the monolayer (i.e. such that increase their X position to $X+a$) are not constrained by the hard-core interactions. Let now $X_0(Y, t)$ denote the X-position of the rightmost particle in the column with fixed Y. Evidently, one has for $\rho_t(X = X_0(Y,t), Y)$ the following equation

$$\begin{aligned}\tau\frac{\mathrm{d}\rho_t(X_0(Y,t),Y)}{\mathrm{d}t} &= -p(X_0(Y,t),Y)\rho_t(X_0(Y,t),Y)\\ &\times\sum_{Y'=Y\pm a}(1-\rho_t(X_0(Y,t),Y'))\\ &-p(X_0(Y,t),Y)\rho_t(X_0(Y,t),Y)\\ &\times(1-\rho_t(X_0(Y,t)-a,Y))\\ &-p(X_0(Y,t),Y)\rho_t(X_0(Y,t),Y)+\\ &+(1-\rho(X_0(Y,t),Y))\\ &\times\Bigg[\sum_{Y'=Y\pm a}p(X_0(Y,t),Y')\rho_t(X_0(Y,t),Y')\\ &+p(X_0(Y,t)+a,Y)\rho_t(X_0(Y,t)+a,Y)\Bigg]\\ &+p(X_0(Y,t)-a,Y) \quad (4)\end{aligned}$$

which thus has a different structure compared to Eq. (3). Note that the last term on the right-hand-side of Eq. (4) is not multiplied by neither the occupation factor $\rho_t(X_0(Y,t),Y)$ nor by the steric factor $(1-\rho_t(X_0(Y,t),Y))$. This happens, namely, because the last term describes the event in which the rightmost particle, present, by definition, at the site $X_0(t)-a$, (i.e. $\rho_t(X_0(Y,t)-a,Y)=1$), hops at the vacant site $X_0(t)$, (i.e. $\rho_t(X_0(Y,t),Y)=0$).

We turn next to the mean-field-type picture assuming first that chemically active sites are uniformly spread along the substrate with mean density α, and $p(X, Y)$ is a position-independent constant

$$p(X,Y) \approx \frac{p_\alpha}{4} \tag{5}$$

An estimate of p_α will be presented below.

Then, we note that the dependences of $\rho_t(X,Y)$ on the X and the Y coordinates have quite different origins. There is a reservoir of particles, which maintains fixed occupation of all sites at $X=0$. Consequently, we may expect a regular X-dependence of $\rho_t(X,Y)$. In contrast, the Y-dependence may be only noise; the uniform boundary at the $X=0$ insures that there is no regular dependence on the Y coordinate and, in absence of disorder in the jump direction probabilities, only the particle dynamics may cause fluctuations in $\rho_t(X,Y)$ along the Y-axis. Hence, following Ref. [6,7] we will disregard these fluctuations and suppose that the local density varies along the X-axis only, i.e. $\rho_t(X,Y)=\rho_t(X)$. Consequently, we will have an effectively one-dimensional problem in which the presence of the Y-direction will be accounted only through the particles' dynamics. We note finally that assumption of such a type is, in fact, quite consistent with experimental observations [2], which show that in case of sufficiently smooth substrates and liquids with low volatility the width of the film's front is very narrow.

Then, in neglect of the fluctuations along the Y-axis the variable $\rho_t(X)$ can be viewed as a local time-dependent variable describing occupation of the site X in a stochastic process in which hard-core particles perform hopping motion (with a time interval τ^* between the consecutive hops) on a one-dimensional lattice of spacing a connected, at the site $X=0$, to a particle reservoir which maintains constant occupation of this site.

For $t \gg \tau$, characteristics of such a process are then described by the following nonlinear system of coupled equations. The mean displacement of the rightmost particle (the monolayer edge) obeys:

$$\tau \frac{\mathrm{d}X_0(t)}{\mathrm{d}t} = \frac{a p_\alpha}{4} \rho_t(X = X_0(t)) \tag{6}$$

where $\rho_t(X)$ is determined by

$$\tau \frac{\partial \rho_t(X)}{\partial t} = \frac{a^2 p_\alpha}{4} \frac{\partial^2 \rho_t(X)}{\partial X^2} \tag{7}$$

which holds for $0 \le X \le X_0(t)$ and is to be solved subject to two boundary conditions:

$$\rho_t(X=0) = 1 \tag{8}$$

and

$$a\tau \frac{\partial \rho_t(X = X_0(t))}{\partial t} = -\frac{a^2 p_\alpha}{4} \frac{\partial \rho_t(X)}{\partial X}\bigg|_{(X = X_0(t))} - \tau \rho_t(X = X_0(t)) \frac{\mathrm{d}X_0(t)}{\mathrm{d}t} \tag{9}$$

These two boundary conditions mimic, first, the presence of a particle reservoir, and second, show that for the rightmost particles of the monolayer the jumps away of the monolayer are not constrained by hard-core interactions.

We note now that Eqs. (6)–(9) constitute a classical mathematical problem of solving a partial differential equation with one of the boundaries being imposed in the moving frame, which is akin to the so-called Stefan problem. Its solution can be found in a standard way by observing that the density profiles $\rho_t(X)$ written in terms of the scaling variable $\omega = X/X_0(t)$ become stationary. In the limit $t \gg \tau$, the mean displacement of the monolayer edge thus follows

$$X_0(t) = \sqrt{2 D_\alpha t \ln\left(\frac{4 D_\alpha t}{\pi a^2}\right)} \tag{10}$$

where D_α is given by

$$D_\alpha = \frac{a^2 p_\alpha}{4\tau} \tag{11}$$

In a similar fashion, one finds that the total number $M(t)$ of particles,

$$M(t) = \int_0^\infty \mathrm{d}X \rho_t(X) \tag{12}$$

emerged on the substrate up to time t, obeys

$$M(t) \sim \sqrt{\frac{4 D_\alpha t}{\pi}} \tag{13}$$

which implies that the mean density in the monolayer slowly decreases with time

$$\overline{\rho_t(X)} = \frac{M(t)}{X_0(t)} \sim \sqrt{\frac{2}{\pi \ln(4 D_\alpha t/\pi a^2)}} \tag{14}$$

Note that dependence of $\overline{\rho_t(X)}$ on disorder, which

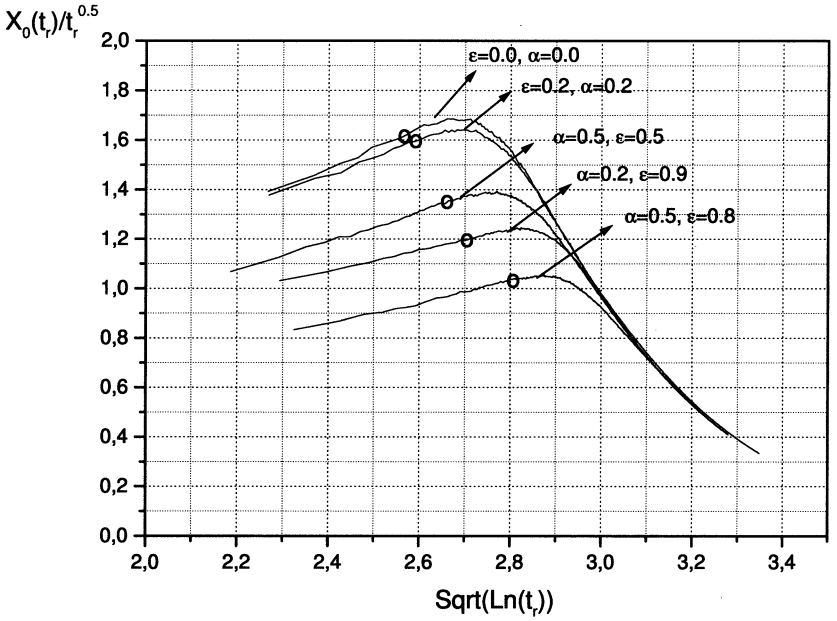

Fig. 2. Plot of $X_0(t)/\sqrt{t}$ vs. $\sqrt{ln(t)}$—numerical evidence for time-dependent logarithmic corrections to the mean displacement of the monolayer edge. Circles denote the time moment when the rightmost particles of the monolayer reach the right edge of the substrate, such that the finite-size effects come into play.

enters only through the effective diffusion coefficient D_α is logarithmically weak. Note also that the mean displacement $X_0(t)$ of the monolayer edge grows at a faster rate than the conventionally expected pure diffusive $\sqrt{t}$-law due to an additional factor $\sqrt{\ln(t)}$; consequently, fitting of experimental curves or numerical results with a pure $\sqrt{t}$-law is meaningless since the effective diffusion coefficient will appear to depend on time of observation. In Fig. 2 we present a numerical evidence of this additional logarithmic factor. In Fig. 3 we depict numerical results describing the behavior of D_α. Analytical estimates of D_α will be presented elsewhere [25].

We finally remark that within the employed mean-field dynamical approach, we can also obtain an average stationary particles current $\langle J_{\text{part}} \rangle$. Solving Eq. (7) subject to the reservoir boundary condition in Eq. (8), as well as imposing a trapping boundary condition at the right edge of the substrate, $\rho_t(X = N) = 0$, we find that

$$\langle J_{\text{part}} \rangle = \frac{D_{\text{J}}}{N} \tag{15}$$

i.e. the current has a Fickian dependence on the substrate's length.

The effective diffusion coefficient D_{J} can be estimated within a mean-field-type approximation as follows: in the stationary state it matters actually how much time, on average, a given particle spends on a given lattice site. Such an average time is, evidently,

$$< \tau > = \tau \times (1 - \alpha) + \tau^* \times \alpha \tag{16}$$

where the first term represents a contribution of ordinary sites, while the second one gives an average time spent by a given particle on chemically active sites. Consequently, the effective diffusion coefficient D_{J} can be estimated as

$$D_{\text{J}} = \frac{a^2}{4 < \tau >} = \frac{a^2}{4\tau} \frac{1 - \varepsilon}{1 - \varepsilon(1 - \alpha)} \tag{17}$$

This result is, of course, exact for $\alpha = 0$ and $\alpha = 1$, i.e. for chemically homogeneous substrates. It appears that it describes reasonably well (see Fig. 4) the numerical data for $\alpha \sim 1$ and arbitrary ε, as well for small values of ε and arbitrary α.

4. Numerical simulations

In our simulation algorithm, we follow closely the model defined in Eq. (2). We consider a square lattice Λ with linear sizes L_x and L_y and with every lattice site (X, Y) we associate an occupation variable $n_{(X, Y)}$ which may assume only two values $\{+1,0\}$. The value $+1$ signifies that the site (X, Y) is occupied, while 0 means that this site is vacant.

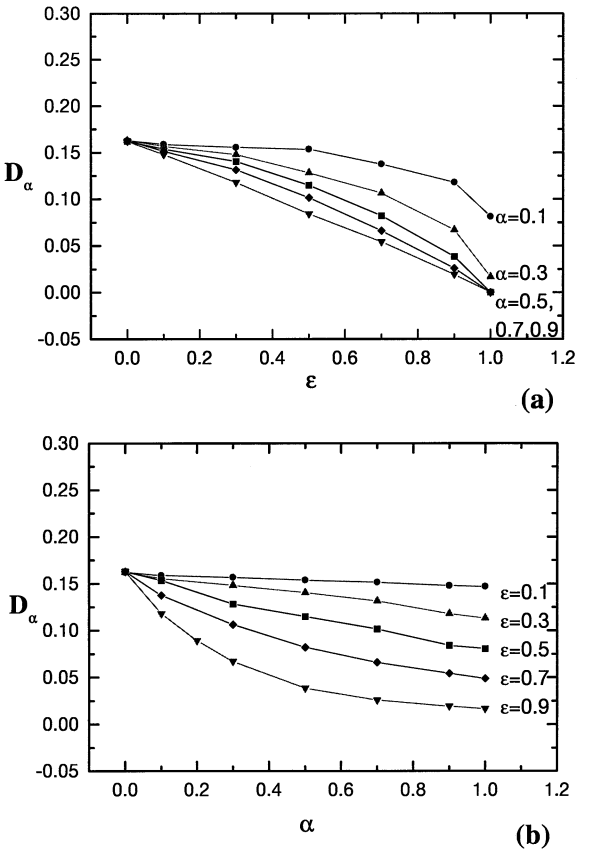

Fig. 3. The dependence of the spreading diffusion coefficient D_α is shown: (a) as a function of the pausing probability ε at different fixed concentrations α of the chemically active sites, solid circles–solid line—$\alpha = 0.1$, solid up-triangles–solid line—$\alpha = 0.3$, solid squares–solid line—$\alpha = 0.5$, solid diamonds–solid line—$\alpha = 0.7$, solid down-triangles–solid line—$\alpha = 0.9$; (b) as a function of the concentration α at different fixed pausing probabilities ε, solid circles–solid line—$\varepsilon = 0.1$, solid up-triangles–solid line—$\varepsilon = 0.3$, solid squares–solid line—$\varepsilon = 0.5$, solid diamonds–solid line—$\varepsilon = 0.7$, solid down-triangles–solid line—$\varepsilon = 0.9$.

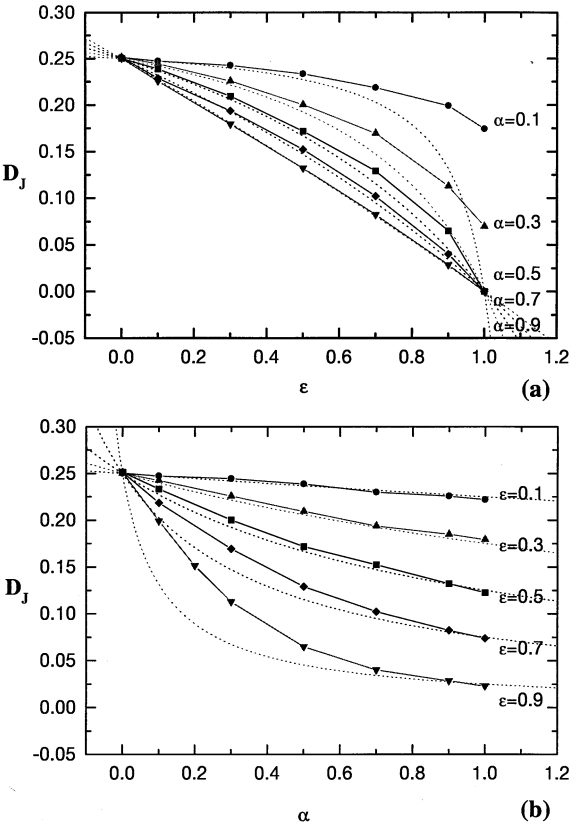

Fig. 4. The dependence of the diffusion coefficient in the stationary state D_J is shown: (a) as a function of the pausing probability ε at different fixed concentrations α of the chemically active sites, solid circles–solid line—$\alpha = 0.1$, solid up-triangles–solid line—$\alpha = 0.3$, solid squares–solid line—$\alpha = 0.5$, solid diamonds–solid line—$\alpha = 0.7$, solid down-triangles–solid line—$\alpha = 0.9$; (b) as a function of the concentration α at different fixed pausing probabilities ε, solid circles–solid line—$\varepsilon = 0.1$, solid up-triangles–solid line—$\varepsilon = 0.3$, solid squares–solid line—$\varepsilon = 0.5$, solid diamonds–solid line—$\varepsilon = 0.7$, solid down-triangles–solid line—$\varepsilon = 0.9$. The dotted lines are the corresponding analytical curves given by Eq. (17).

The initial configuration is an empty lattice except for the zeroth raw ($X = 0$). The left edge of the system $X = 0$ is coupled to a particle reservoir which keeps the zeroth raw always occupied ($C_0 = 1$), i.e. $\{n_{(0, Y)} \equiv 1, \quad Y = 1,\cdots,L_y\}$. In the Y-direction periodic boundary conditions are imposed to reduce the finite-size effects. The right edge of the system is coupled to an empty reservoir, so that the raw $\{X = L_x + 1\}$ is always empty. Note that such a formulation allows us to

study both dynamic and static characteristics. While studying spreading dynamics, we take L_x sufficiently large and take care that displacement of the rightmost particle in each column Y is less than $L_x + 1$. When studying the behavior of the stationary particle current, we focus on L_x not that large and let the system evolve until the density profiles in the system attain a stationary state.

The following time-saving procedure has been implemented. At every non-normalized time step i a particle in the system is chosen at random. Let the particle's coordinates be denoted by (X, Y). Then the particle may either stay at the site (X, Y) with probability $\varepsilon(X,Y)\{=\varepsilon,0\}$, or with an equal probability, $p(X,Y) = (1-\varepsilon(X,Y))/4$, may attempt to jump onto one of the neighboring sites, chosen at random. The jump is actually fulfilled if the target site is empty. Otherwise, the particle remains at the site (X, Y). If the initial site is in the zeroth raw and if after the update the particle moves it is immediately filled by a particle from the reservoir and the number of particles N_i in the system is increased. If the initial site is in the last raw $X = L_x$ and if after the update the particle moves to $X' = L_x + 1$ the number of particles in the system is decreased. The time is renormalized according to

$$t_{i+1} = t_i + \frac{1}{N_{i+1}} \tag{18}$$

where N_{i+1} is the total number of particles in the system at the non-normalized time $(i+1)$. We use the averaged renormalized time in our studies of the time-dependent quantities.

Most of the simulations are performed for a system of size 100×25, 200×50 and 100×100 in units of the lattice constant a. Larger system sizes are also considered in few cases. The results are usually averaged over $N_s = 2$, 5, 10 different substrates and for each substrate $N_r = 5$, 10 different runs are performed. Typical Monte Carlo simulation lasted $1.6 \div 2 \times 10^5$ MCS per site.

5. Simulation results

After passing through a transient regime the system reaches a stationary non-equilibrium state characterized by a stationary average particle current J_{part} flowing through the system and a constant average density gradient.

We studied here how do both, the spreading diffusion coefficient D_α and the diffusion coefficient in the stationary state D_J, depend on the pausing probability ε and on the concentration α of the chemically active sites. The spreading diffusion coefficient D_α was determined from the time dependence of the average interface position $X_0(t)$ before particles start leaving the right edge of the system. It appears that the law in Eq. (10) describes very well the time behavior of the average interface position not only for $\alpha = 0, \quad \varepsilon = 0$ [6,7], but also for practically the whole interval of values of α and ε, except at $\varepsilon = 1.0$, i.e. infinitely deep trapping sites (see Fig. 2).

For determination of the diffusion coefficient D_J in the stationary state we use Fick's law, $J_{\mathrm{part}} = -D_J \nabla\rho$, by measuring the average particle current, J_{part} (per site), and the average density gradient, $\nabla\rho(\approx \text{const.})$, in the stationary state at given pausing probability ε and concentration α. The obtained results for the spreading diffusion coefficient D_α are presented in Fig. 3 and the corresponding results for the diffusion coefficient D_J in the stationary state are given in Fig. 4. Curiously enough, the values found for D_α are always lower then those obtained for D_J.

We turn now to the special case when the pausing probability on chemically active sites is $\varepsilon = 1$. The specific feature of this case is that the particle, once arriving at any chemically active site stays there forever, serving then as impenetrable obstacle for the other particles. It means that in this case one has an induced percolative behavior. The time behavior of the average interface position for $\alpha > 0.1$ is no longer fitted well by the function in Eq. (10) (one expects that here a logarithmic time behavior should take place) and the above mentioned method cannot be employed to determine the spreading diffusion coefficient D_α. For given α the averaged density distribution in the stationary state is still constant and $\nabla\rho \approx -(1-\alpha)/L_x$. In order to get a reliable estimates for the studied quanitities (e.g. the particle current J_{part}) the demand on the computing time as the

concentration $\alpha \to \alpha_c$ increases significantly since longer time runs are necessary as well as averaging over more substrates is needed and finally also bigger systems should be simulated. The approximate value found for the concentration $\alpha_c \approx 0.4 \pm 0.01$ at which the particle current J_{part} (respectively D_J) turns to zero is consistent with $1 - p_c$, where $p_c = 0.592746$ [44] is the critical probability for site percolation in the square lattice (see Fig. 5).

6. Monolayer of interacting particles.

We turn finally to the case when the monolayer particles experience short-range (nearest-neighbor) attractive interactions. Let us consider the simplest possible case when the corresponding Hamiltonian is

$$H = -U \sum_{(X',Y')} n(X,Y)n(X',Y'), \tag{19}$$

where U $(U > 0)$ is the constant describing the attraction between two diffusing particles and the summation symbol with the subscript (X',Y') means that summation extends over the sites (X',Y'), neighbouring to the site (X,Y). We still assume the activation mechanism for the hopping motion of the monolayer particles; that is, the probability for jump depends on the trapping energy of the site (X, Y) through:

$$P_{jump}(X,Y) = \exp\left(\frac{U_{tr}(X,Y)}{k_B T}\right)$$

We take into consideration the interaction between the diffusing particles by assuming that the particle 'feels' the other particles when choosing the direction for the jump, i.e.:

$$P_{dir}((X,Y),(X',Y')) = \frac{1}{Z}\exp\left(\frac{-\Delta H((X,Y),(X',Y'))}{2K_B T}\right),$$

$$Z = \sum_{(X',Y')} P_{dir}((X,Y),(X',Y'))$$

where

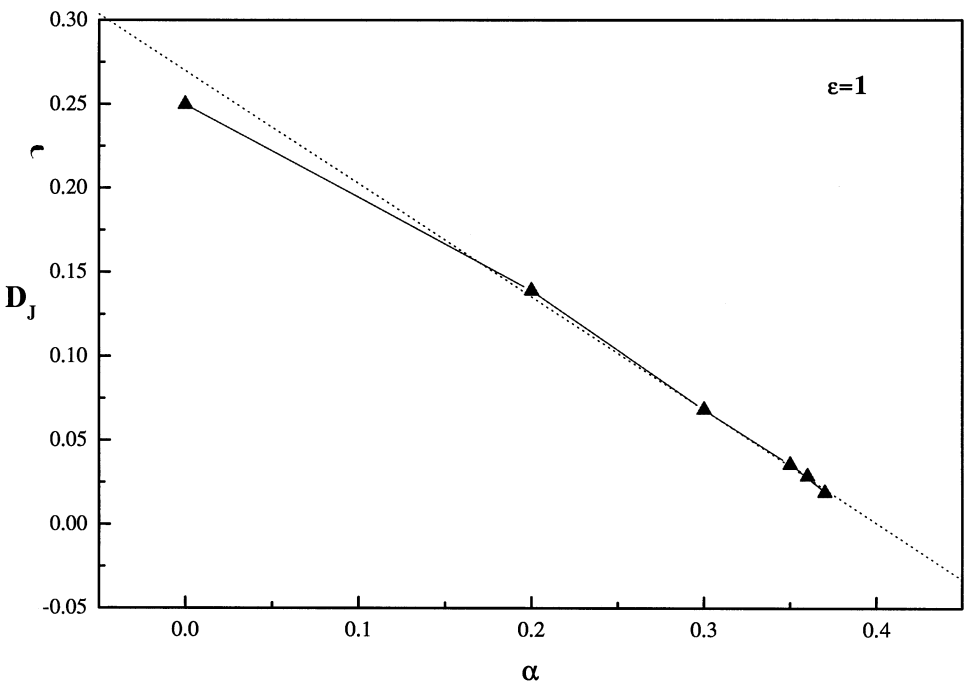

Fig. 5. Percolation threshold. The plot of D_J vs. α for $\varepsilon = 1$. Linear extrapolation of the numerical data gives the critical value of $\alpha = \alpha_c$ at which the current vanishes equal to $\alpha_c \approx 0.4 \pm 0.01$.

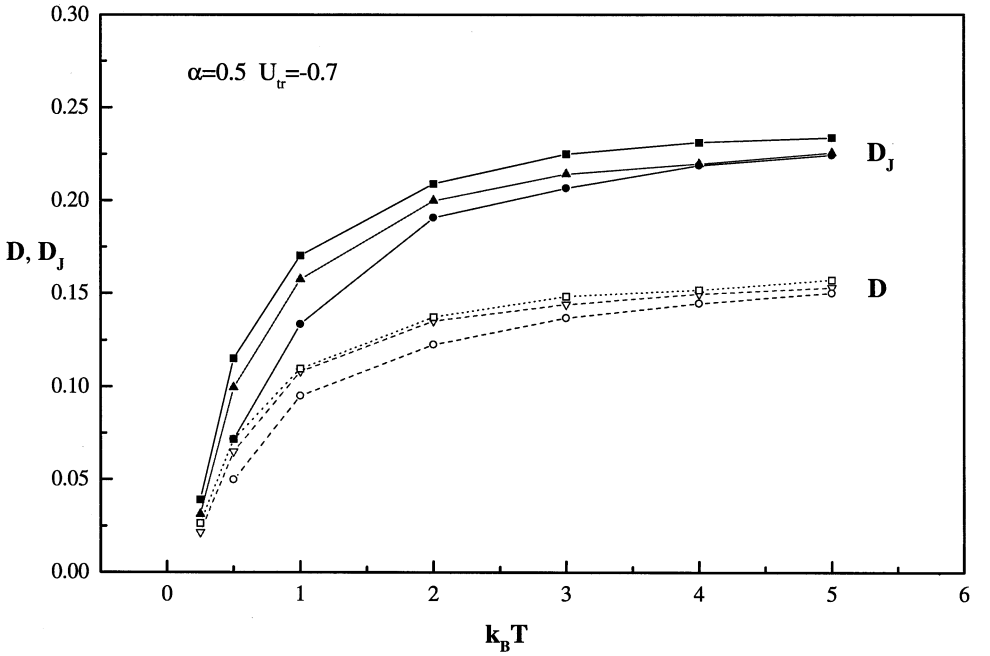

Fig. 6. The temperature dependence of the spreading diffusion coefficient D_α and the diffusion coefficient D_J in the stationary state. Concentration of the chemically active sites is $\alpha = 0.5$ of the trapping sites and their trapping energy U_{tr} is taken equal to $U_{tr} = -0.7$. For the non-interacting system ($U = 0$) the results for D_J and for D_α are given by solid squares–solid lines and by open squares–dotted line, respectively. For the weakly (compared to the trapping energy) interacting system ($U = 0.1$)—solid up-triangles–solid line and open up-triangles–dotted line depict, respectively, the behavior of D_J and D_α. For ($U = 0.3$)—solid circles–solid line define D_J, while open circles–dashed line determine the corresponding behavior of the spreading diffusion coefficient D_α.

$\Delta H((X,Y),(X',Y')) = H(X',Y') - H(X,Y)$ and $H(X,Y) = -U\, n(X,Y)\Sigma_{(X',Y')} n(X',Y')$ is the interaction energy of the particle at the site (X, Y).

For high enough temperatures one may, as a first approximation, try to determine the diffusion coefficients D_α and D_J in the same way as it was done for the non-interacting system. The temperature dependence of the diffusion coefficients determined in this way is shown in Fig. 6. As could be seen taking into consideration the interaction between the diffusing particles leads to a decrease of the diffusion coefficients. For higher temperatures the effect is less pronounced.

For lower temperatures another method for determining D_J should be employed. While for lower temperatures the time behavior of the average interface position $X_0(t)$ is still reasonably well described by Eq. (10), the density distribution along the spreading direction in the stationary state is no longer linear. In Fig. 7 the corresponding density distributions (for homogeneous substrate, $\alpha = 0$, $U_{tr} = 0$) are shown for three different temperatures for the interacting system in the stationary state. One can see that at $k_B T = 0.5U$ there is clearly a phase separation though there is a stationary particle current flowing through the system. The interface between the two phases is approximately at $X = L_x/2$. At higher temperatures, e.g. $k_B T = 2.5U$ the density distribution is getting closer to a linear distribution (as in the non-interacting case) but is still not linear. This system is very similar to the driven diffusive system introduced by Katz et al. [45,46] where there is a stationary particle current flowing in the system due to a bias in the transition rates.

7. Conclusions

To conclude, we have studied the spreading kinetics of a monolayer of hard-core particles on

a semi-infinite, chemically heterogeneous solid substrate, one side of which is attached to a reservoir of particles. The substrate is modeled as a square lattice containing two types of sites-ordinary ones and special, chemically actives sites placed at random positions with mean concentration α. These special sites temporarily immobilize the particles of the monolayer which then serve as impenetrable obstacles for the other particles. In terms of a mean-field-type theory, we have shown that the mean displacement $X_0(t)$ of the monolayer edge grows with time t as $X_0(t) = \sqrt{2D_\alpha t \ln(4D_\alpha t/\pi a^2)}$, ($a$ being the lattice spacing). This nontrivial time dependence is confirmed by the numerical simulations. For a broad range of values of α and of the trapping times of the chemically active sites (pausing probabilities) D_α has been obtained from extensive Monte Carlo simulations. In addition, we have studied numerically the behavior of the stationary particle current in finite samples. We have observed that, curiously enough, the diffusion coefficient D_α deduced from the analysis of the data on the spreading kinetics, and the one obtained from the analysis of the data on the stationary particle currents, D_J, are different from each other and obey $D_\alpha < D_J$. Besides, we have found that the system displays a percolation-type behavior when $\varepsilon = 1$ and $\alpha \to \alpha_c \approx 0.4 \pm 0.01$. In this limiting case both D_α and D_J vanish. The question of the influence of attractive particle–particle interactions on spreading kinetics has been also addressed. We have observed that taking into consideration attractive interactions between the diffusing particles leads to a decrease of the diffusion coefficients. For higher temperatures the effect becomes less pronounced, as it should. Finally, we have found that for sufficiently strong attractions the density distribution along the spreading direction in the stationary state is no longer linear and that there is clearly a phase separation, though the stationary particle current does not vanish.

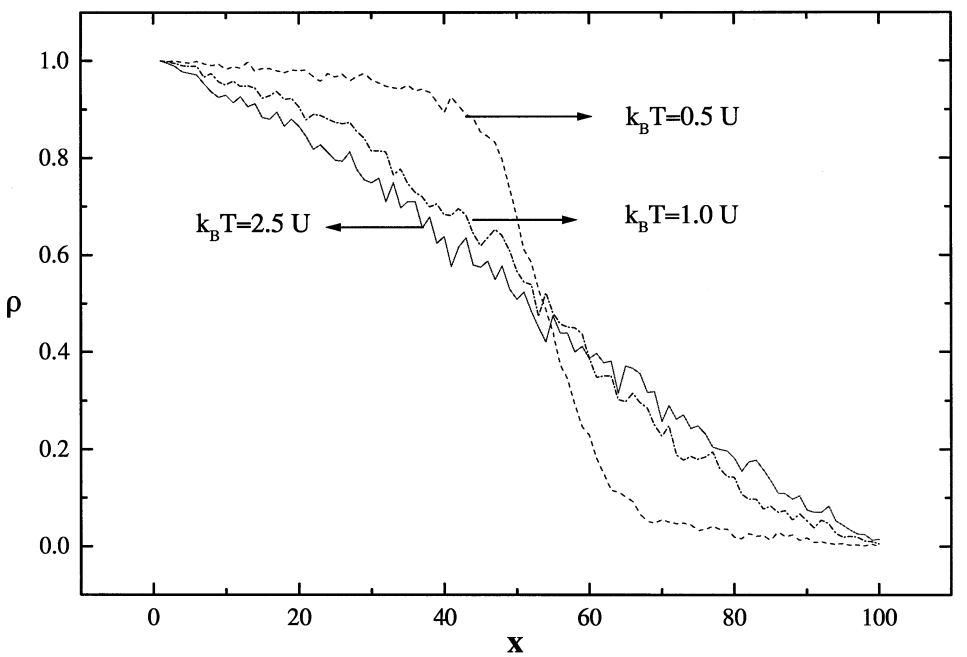

Fig. 7. The average density distributions along the spreading direction X in homogeneous systems ($\alpha = 0$ and $U_{tr} = 0$) are shown for the interacting ($U = 1$) system 100×25 (in units of the lattice constant) in the stationary state at three different temperatures: $k_B T = 2.5U$ solid line, $k_B T = 1U$ dashed line, $k_B T = 0.5U$ dotted line.

Acknowledgements

The authors thank M. Voué and J. De Coninck for fruitful discussions and interest to this work. We also wish to thank M. Voué for his help in preparing the preliminary simulation codes.

References

[1] A.W. Adamson, Physical Chemistry of Interfaces, 5th ed., Wiley, New York, 1990.
[2] A.M. Cazabat, Contemp. Phys. 28 (1987) 347.
[3] S. Granick, Science 253 (1991) 1734.
[4] L. Léger, J.F. Joanny, Rep. Prog. Phys. 72 (1992) 431.
[5] S. Dietrich, in: C. Domb, J.L. Lebowitz (Eds.), Phase Transitions and Critical Phenomena, vol. 10, Academic Press, London, 1988, p. 1.
[6] S.F. Burlatsky, G. Oshanin, A.M. Cazabat, M. Moreau, Phys. Rev. Lett. 76 (1996) 86.
[7] S.F. Burlatsky, G. Oshanin, A.M. Cazabat, M. Moreau, Phys. Rev. E 54 (1996) 3832.
[8] G. Oshanin, J. De Coninck, A.M. Cazabat, M. Moreau, Phys. Rev. E 58 (1998) R20.
[9] H. Gau, S. Herminghaus, P. Lenz, R. Lipowski, Science 283 (1999) 46.
[10] D.E. Kataoka, S.M. Troian, Nature (London) 402 (1999) 794.
[11] C.S. Chen, M. Mrksich, S. Huang, G.M. Whitesides, D.E. Ingber, Science 276 (1997) 1425.
[12] E. Delamarche, A. Bernard, H. Schmidt, B. Michel, H.A. Biebuyck, Science 276 (1997) 779.
[13] S. Curtarolo, M.J. Bojan, G. Stan, M.W. Cole, W.A. Steele, Proceedings of 2nd Pacific Basin Conference on Adsorption Science and Technology, Brisbane, Australia, May 2000.
[14] P.S. Swain, R. Lipowsky, Langmuir 14 (1998) 6772.
[15] C. Bauer, S. Dietrich, Phys. Rev. E 60 (1999) 6919.
[16] D. Urban, K. Topolski, J. De Coninck, Phys. Rev. Lett. 76 (1996) 4388.
[17] T.W. Burkhardt, J. Phys. A 31 (1998) L549.
[18] M. Schoen, D.J. Diestler, Phys. Rev. E 56 (1997) 4427.
[19] L.J. Douglas Frink, A.G. Salinger, J. Chem. Phys. 110 (1999) 5669.
[20] D.J. Olbris, A. Ulman, Y. Schnidman, J. Chem. Phys. 102 (1995) 6865.
[21] M.H. Adão, M. de Ruijter, M. Voué, J. De Coninck, Phys. Rev. E 59 (1999) 746.
[22] M. Voué, S. Semal, J. De Coninck, Langmuir 15 (1999) 7855.
[23] M.P. Valignat, G. Oshanin, S. Villette, A.M. Cazabat, M. Moreau, Phys. Rev. Lett. 80 (1998) 5377.
[24] M. Voué, M.P. Valignat, G. Oshanin, A.M. Cazabat, Langmuir 15 (1999) 1522.
[25] N. Pesheva, G. Oshanin, in preparation.
[26] O. Bénichou, J. Klafter, M. Moreau, G. Oshanin, Phys. Rev. E 62 (2000) 3327.
[27] O. Bénichou, G. Oshanin, Phys. Rev. E 64 (2001) R020103.
[28] O. Bénichou, A.M. Cazabat, J. De Coninck, M. Moreau, G. Oshanin, Phys. Rev. Lett. 84 (2000) 511.
[29] O. Bénichou, A.M. Cazabat, J. De Coninck, M. Moreau, G. Oshanin, Phys. Rev. B 63 (2001) 235413.
[30] O. Bénichou, A.M. Cazabat, J. De Coninck, M. Moreau, G. Oshanin, J. Phys. C 13 (2001) 4835.
[31] H.J. Kreuzer, Diffusion at Interfaces: Microscopic Concepts, Springer Series in Surface Science, vol. 12, Springer–Verlag, Berlin, 1986.
[32] R. Gomer, Rep. Prog. Phys. 53 (1990) 917.
[33] J.W. Haus, K.W. Kehr, Phys. Rep. 150 (1987) 263.
[34] K.W. Kehr, T. Wichmann, Diffusion coefficients of single and many particles in lattices with different forms of disorder, in: Proceedings of the International Seminar on Current Developments in Disordered Materials, Kurukshetra University, India, 22–24 January, 1996.
[35] S. Vasenkov, J. Kärger, D. Freude, R.A. Rakoczy, J. Weitkamp, J. Mol. Catal. A 158 (2000) 373.
[36] M.-O. Coppens, A.T. Bell, A.K. Chakraborty, Chem. Eng. Sci. 54 (1999) 3455.
[37] J. Hinderer, F.J. Keil, Chem. Eng. Sci. 51 (1996) 2667.
[38] A. Clark, The Theory of Adsorbtion and Catalysis, Academic Press, New York, 1970.
[39] J.J. McAlpin, R.A. Pierotti, J. Chem. Phys. 41 (1964) 68.
[40] J.J. McAlpin, R.A. Pierotti, J. Chem. Phys. 42 (1965) 1842.
[41] A.F. Devonshire, Proc. Roy. Soc. (Lond.) Ser. A 163 (1937) 132.
[42] A. Zangwill, Physics at Surfaces, Cambridge University Press, Cambridge, 1988.
[43] S. Ramaswamy, G. Mazenko, Phys. Rev. A 26 (1982) 1735.
[44] R.M. Ziff, B. Sapoval, J. Phys. A 19 (1987) L1169.
[45] S. Katz, J.L. Lebowitz, H. Spohn, Phys. Rev. B 28 (1983) 1655.
[46] S. Katz, J.L. Lebowitz, H. Spohn, J. Stat. Phys. 34 (1984) 497.